QUADRATURE RULE FOR SINGULAR INTEGRALS IN COMMON ENGINEERING PROBLEMS

ROCÍO VELÁZQUEZ MATA, ANTONIO ROMERO ORDÓÑEZ & PEDRO GALVÍN BARRERA
Escuela Técnica Superior de Ingeniería, Universidad de Sevilla, Spain

ABSTRACT
This paper describes a general method to compute the boundary integral equation for common engineering problems. The proposed procedure consists of a new quadrature rule to evaluate singular and weakly singular integrals. The methodology is based on the computation of the quadrature weights by solving an undetermined system of equations in the minimum norm sense. The Bézier–Bernstein form of a polynomial is also implemented as an approximation basis to represent both geometry and field variables. Therefore, exact boundary geometry is considered, and arbitrary high-order elements are allowed. This procedure can be used for any element node distribution and shape function. The validity of the method is demonstrated by solving a two-and-a-half-dimensional elastodynamic benchmark problem.
Keywords: boundary integral equation, singular kernels, numerical integration, Bernstein polynomials, Bézier curve, 2.5D formulation.

1 INTRODUCTION

The Boundary Element Method (BEM) allows solving several engineering problems such as acoustic scattering, fracture mechanics, soil wave propagation, and heat transfer with high accuracy and efficiency [1]. The BEM is based on the fundamental solution of a particular problem that is used as weighting function and allows one to eliminate the domain discretization. Then, the methodology results in boundary integral equations (BIE) for a point $\mathbf{x}^*$ located at the arbitrary boundary Γ as follows [2]:

$$c(\mathbf{x}^*)u(\mathbf{x}^*) = \int_\Gamma \left(t(\mathbf{x})\mathcal{G}(\mathbf{x},\mathbf{x}^*) - u(\mathbf{x})\mathcal{H}(\mathbf{x},\mathbf{x}^*)\right)\, d\Gamma(\mathbf{x})\,, \tag{1}$$

where $\mathbf{x}^*$ is the collocation point, $u(\mathbf{x})$ and $t(\mathbf{x})$ are the field variables, $\mathcal{G}(\mathbf{x},\mathbf{x}^*)$ and $\mathcal{H}(\mathbf{x},\mathbf{x}^*)$ are the fundamental solutions at point $\mathbf{x}$ due to a point source located at $\mathbf{x}^*$, and the integral-free term $c(\mathbf{x}^*)$ depends only on the boundary geometry at the collocation point [2]. The fundamental solution is chosen according to the actual problem. In addition, the boundary discretization is determined by the fundamental solution.

Eqn (1) allows computing the solution to many problems. The integrals in eqn (1) should be understood in the sense of the Cauchy Principal Value (CPV). These integrals can be regular, near-singular, weak-singular, singular, or hypersingular integrals, depending on the problem studied. Regular integrals are integrated by Gaussian quadrature. In the rest of the cases, their analytical evaluation depends on the fundamental solution and the shape functions used to approximate the field variables at the boundary element. Both parameters determine the difficulty of the procedure.

In previous works, specific developments were done to obtain the CPV of the integrals involving the corresponding problems. This research describes a general procedure that allows computing the BIE for common engineering problems using numerical quadratures. The methodology is based on the computation of the weights of the quadrature rules by the solution of an underdetermined system of equations in the minimum norm sense as in Carley [3]. The equations are obtained from the finite part of integral kernels including

the element shape functions evaluated at the quadrature points to increase the accuracy. Bernstein polynomials are taken into account to develop this general approach since Lagrange polynomials can be obtained from a Bernstein base. The proposed method can be used for any element and shape function. The performance of the quadrature rules is evaluated in the BEM formulation based on the Bézier–Bernstein space [4], which allows the exact boundary geometry representation.

The paper is organized as follows. First, the numerical model is presented. The quadrature rules are discussed, and the accuracy in the computation of integral kernels for different element families and order is shown. The proposed method is then verified using a benchmark problem consisting of an elastic cavity in two-and-a-half dimensions (2.5D). Finally, the conclusion section summarizes the main contributions of this work.

2 NUMERICAL APPROACH

The starting point for the formulation of the BEM is the BIE (eqn (1)). The meaning of these variables depends on the formulation of the physical problem under study.

The boundary is discretized into N elements, $\Gamma = \bigcup_{j=1}^{N} \Gamma^j$, and the field variables within an element Γ^j are approximated from the nodal values u^i and t^i through the element shape functions $\phi^i(\mathbf{x})$ of order p. Thus, eqn (1) is rewritten as follows:

$$c(\mathbf{x}^*)u(\mathbf{x}^*) = \sum_{j=1}^{N}\sum_{i=1}^{p}\left[\left(\int_{\Gamma^j}\phi^i(\mathbf{x})\mathcal{G}(\mathbf{x},\mathbf{x}^*)\,d\Gamma\right)t^i - \left(\int_{\Gamma^j}\phi^i(\mathbf{x})\mathcal{H}(\mathbf{x},\mathbf{x}^*)\,d\Gamma\right)u^i\right]. \quad (2)$$

The behavior of the element integration kernels depends on the radius $||\mathbf{x}-\mathbf{x}^*||$ and leads to regular, near singular, and singular integrals. The first two types are easily integrated by ordinary Gauss–Legendre quadrature, using a smoothing transformation to handle near-singular behavior. However, the singular kernels must be correctly integrated.

2.1 Quadrature rules

The fundamental solution to common engineering problems (such as elastostatic, acoustic, elastodynamic, heat transfer, among others) includes weakly singular and singular terms of the form $\log|\mathbf{x}^*-\mathbf{x}|$ and $1/(\mathbf{x}^*-\mathbf{x})$. Moreover, the series expansion of the fundamental solution includes some of these terms for null radius. Although the logarithmic singularity can be integrated by quadratures such as those proposed in Monegato and Scuderi [5], the other type must be interpreted as the CPV. Hypersingular kernels are not considered in this work. Kolm and Rokhlin [6] and Carley [3] proposed quadrature rules based on integrals of Legendre polynomials of order n.

The design of the new quadrature rules considers the integral of the element shape function instead of the Legendre polynomials. We use the Lagrange interpolant of arbitrary order p as the element shape function. The proposed method is valid for any element node distribution, such as equidistant nodes, Legendre–Gauss–Lobatto (LGL) integration points used in the spectral formulations [7], or simpler distributions such as the family of Chebyshev points [4]. The generality of the proposed method is achieved because the Lagrange interpolant can be derived from the Bernstein basis as:

$$\phi^i(t) = \sum_{k=0}^{n} c_k^i B_k^n(t), \quad (3)$$

where c_k^i are control points and $B_k^n(t)$ is the Bernstein basis of degree n defined over the interval $t \in [0,1]$ as:

$$B_k^n(t) = \binom{n}{k} t^k (1-t)^{n-k}, \quad k = 0, \ldots, n. \tag{4}$$

The Lagrange interpolant derived from the Bernstein basis must fulfill the following condition at the element nodes t_j:

$$\phi^i(t_j) = \sum_{k=0}^{n} c_k^i B_k^n(t_j) = \delta_{ij}, \qquad j = 0, \ldots, n. \tag{5}$$

This condition is commonly expressed as a linear system of equations through the Bernstein–Vandermonde matrix $A_{ij} = B_i^n(t_j)$ as:

$$\begin{bmatrix} B_0^n(t_0) & B_1^n(t_0) & \ldots & B_k^n(t_0) & \ldots & B_n^n(t_0) \\ B_0^n(t_1) & B_1^n(t_1) & \ldots & B_k^n(t_1) & \ldots & B_n^n(t_1) \\ \ldots & & & & & \\ B_0^n(t_j) & B_1^n(t_j) & \ldots & B_k^n(t_j) & \ldots & B_n^n(t_j) \\ \ldots & & & & & \\ B_0^n(t_n) & B_1^n(t_n) & \ldots & B_k^n(t_n) & \ldots & B_n^n(t_n) \end{bmatrix} \begin{Bmatrix} c_0^i \\ c_1^i \\ \ldots \\ c_k^i \\ \ldots \\ c_n^i \end{Bmatrix} = \begin{Bmatrix} 0 \\ 0 \\ \ldots \\ 1 \\ \ldots \\ 0 \end{Bmatrix}. \tag{6}$$

Thus, the element shape function ϕ^i is defined by the control points obtained from the solution of eqn (6).

The definition of the shape function on Bernstein basis allows the design of the quadrature rules for singular integrals in eqn (2) as:

$$\begin{aligned} \int_{-1}^{1} \phi^i(\xi) \mathcal{G}(\xi, \mathbf{x}^*) \frac{d\Gamma}{d\xi} \, d\xi &= \int_0^1 \phi^i(t) \mathcal{G}(t, \mathbf{x}^*) \frac{d\Gamma}{d\xi} \frac{d\xi}{dt} \, dt \\ &= \int_0^1 \left(\sum_{k=0}^{n} c_k^i B_k^n(t) \right) \mathcal{G}(t, \mathbf{x}^*) \frac{d\Gamma}{d\xi} \frac{d\xi}{dt} \, dt \\ &= \sum_{k=0}^{n} c_k^i \left(\int_0^1 B_k^n(t) \mathcal{G}(t, \mathbf{x}^*) \frac{d\Gamma}{d\xi} \frac{d\xi}{dt} \, dt \right), \end{aligned} \tag{7}$$

where $t = (\xi + 1)/2$.

The quadrature rules should be able to compute integrals accounting the terms of the fundamental solutions or its series expansion:

$$\int_{-1}^{1} B_k^n(\xi) \, d\xi = \int_0^1 B_k^n(t) \frac{d\xi}{dt} \, dt, \tag{8}$$

$$\int_{-1}^{1} B_k^n(\xi) \log|\xi^* - \xi| \, d\xi = \int_0^1 B_k^n(t) \log|\xi^* - 2t + 1| \frac{d\xi}{dt} \, dt, \tag{9}$$

$$\text{PV} \int_{-1}^{1} \frac{B_k^n(\xi)}{\xi^* - \xi} \, d\xi = \text{PV} \int_0^1 \frac{B_k^n(t)}{\xi^* - 2t + 1} \frac{d\xi}{dt} \, dt, \quad k = 0, \ldots, n, \tag{10}$$

where ξ^* is the element natural coordinate of the collocation point $\mathbf{x}^*$, and PV makes reference to Cauchy principal value.

The quadrature rule of order M approximates the integral of $f(\xi, \xi^*)$ as:

$$\int_{-1}^{1} f(\xi, \xi^*)\, d\xi = \int_{0}^{1} f(t, \xi^*) \frac{d\xi}{dt}\, d\xi \simeq \sum_{m=0}^{M} f(t_m, \xi^*) \frac{d\xi}{dt} w_m, \tag{11}$$

where $f(t_m, \xi^*)$ represents the integral kernels in eqns (8)–(10) evaluated at the integration point t_m, and w_m are the quadrature weights.

Eqns (8)–(10) and eqn (11), evaluated as an equality, allow to define a system of $3(n+1)$ equations with $M+1$ unknowns that represent the weights of the quadrature rule. The number of equations is given by the three types of integrals and the $n+1$ polynomials. Each equation is related to the integrals defined in eqns (8)–(10) for the Bernstein polynomial $B_k^n(t)$. Thus, the following system of equations is obtained:

$$\begin{bmatrix} \psi_0(t_0,\xi^*) & \psi_0(t_1,\xi^*) & \dots & \psi_0(t_m,\xi^*) & \dots & \psi_0(t_M,\xi^*) \\ \psi_1(t_0,\xi^*) & \psi_1(t_1,\xi^*) & \dots & \psi_1(t_m,\xi^*) & \dots & \psi_1(t_M,\xi^*) \\ \dots & & & & & \\ \psi_k(t_0,\xi^*) & \psi_k(t_1,\xi^*) & \dots & \psi_k(t_m,\xi^*) & \dots & \psi_k(t_M,\xi^*) \\ \dots & & & & & \\ \psi_n(t_0,\xi^*) & \psi_n(t_1,\xi^*) & \dots & \psi_n(t_m,\xi^*) & \dots & \psi_n(t_M,\xi^*) \end{bmatrix} \begin{Bmatrix} w_0 \\ w_1 \\ \dots \\ w_m \\ \dots \\ w_M \end{Bmatrix} = \begin{Bmatrix} m_0 \\ m_1 \\ \dots \\ m_k \\ \dots \\ m_n \end{Bmatrix}, \tag{12}$$

where,

$$\psi_k(t_m, \xi^*) = \begin{bmatrix} B_k^n(t_m) \dfrac{d\xi}{dt} \\ B_k^n(t_m) \log|\xi^* - 2t_m + 1| \dfrac{d\xi}{dt} \\ \dfrac{B_k^n(t_m)}{\xi^* - 2t_m + 1} \dfrac{d\xi}{dt} \end{bmatrix}, \tag{13}$$

$$m_k = \begin{Bmatrix} \int_0^1 B_k^n(t) \dfrac{d\xi}{dt}\, dt \\ \int_0^1 B_k^n(t) \log|\xi^* - 2t + 1| \dfrac{d\xi}{dt}\, dt \\ \text{PV} \int_0^1 \dfrac{B_k^n(t)}{\xi^* - 2t + 1} \dfrac{d\xi}{dt}\, dt \end{Bmatrix}. \tag{14}$$

The generalized moments m_i are obtained from the Brandaõ approach to the finite-part integrals [8] according to Carley [3].

In the case of an undetermined system of equations, the integration weights are obtained as the solution of eqn (12) in the minimum norm least-squares sense. The Jacobian $d\xi/dt$ in eqn (11) can be included in the integration weights to use the integration points ξ_m defined in $[-1, 1]$ instead of t_m at $[0, 1]$.

2.1.1 Numerical verification

The quadrature rule is verified by the integration of the following integrals:

$$I_1 = \int_{-1}^{1} \phi^i(\xi)\, d\xi, \tag{15}$$

$$I_2 = \int_{-1}^{1} \phi^i(\xi) \log|\xi^* - \xi|\, d\xi, \tag{16}$$

$$I_3 = \mathrm{PV} \int_{-1}^{1} \frac{\phi^i(\xi)}{\xi^* - \xi}\, d\xi. \tag{17}$$

The exact value of these integrals can be computed from eqn (7) using the moments in eqn (14).

Fig. 1 shows the L_2 scaled error ϵ_2 in the computation of integral in eqns (15)–(17) for different element order and node distributions: (i) Chebyshev points of the first kind; (ii) Chebyshev points of the second kind; (iii) LGL integration points; and (iv) equidistant nodes [4]. The accuracy of the proposed quadrature rules is analyzed for different numbers of integration points M according to the shape function order p. The integration error increases with the order of the element p, and is slightly affected by the number of integration points for $M \geq 4(p+1)$. The quadrature rule did not give accurate results for $M = 2(p+1)$. A quadrature rule of order $4(p+1)$ is adequate to solve the singular integrals in common engineering problems considered in this paper.

2.2 The BEM formulation in the Bézier–Bernstein space

In this work, the BEM formulation in the Bézier–Bernstein space [4], [9] is used to show the performance of the proposed quadrature rules. It is based on the application of polynomials in Bernstein form for the definition of Bézier curves $\mathbf{r}_n(t)$:

$$\mathbf{r}_n(t) = \sum_{k=0}^{n} \mathbf{b}_k B_k^n(t), \tag{18}$$

where $\mathbf{b}_k$ are the control points used to approximate the geometry and n is the degree of the curve. An efficient curve computation is achieved using the polar form (or blossom) of a Bézier curve $\mathbf{r}_n(t)$ [10], which defines a multi-affine transformation satisfying:

$$\mathbf{b}_k = \mathbf{R}(\underbrace{0,\ldots,0}_{n-k},\underbrace{1,\ldots,1}_{k}), \tag{19}$$

where $\mathbf{R}(t_1,\ldots,t_n)$ is computed as:

$$\mathbf{R}(t_1,\ldots,t_n) = \sum_{\substack{I\cap J=\emptyset \\ I\cup J=\{1,2,\ldots,n\}}} \prod_{i\in I}(1-t_i) \prod_{j\in J} t_j \mathbf{b}_{|J|}, \tag{20}$$

Thus, a polynomial in Bernstein form can be formulated in the polar form, substituting eqn (19) into eqn (18) as follows:

$$\mathbf{r}_n(t) = \sum_{k=0}^{n} \mathbf{R}(\underbrace{0,\ldots,0}_{n-k},\underbrace{1,\ldots,1}_{k}) B_k^n(t) = \mathbf{R}(t,\ldots,t). \tag{21}$$

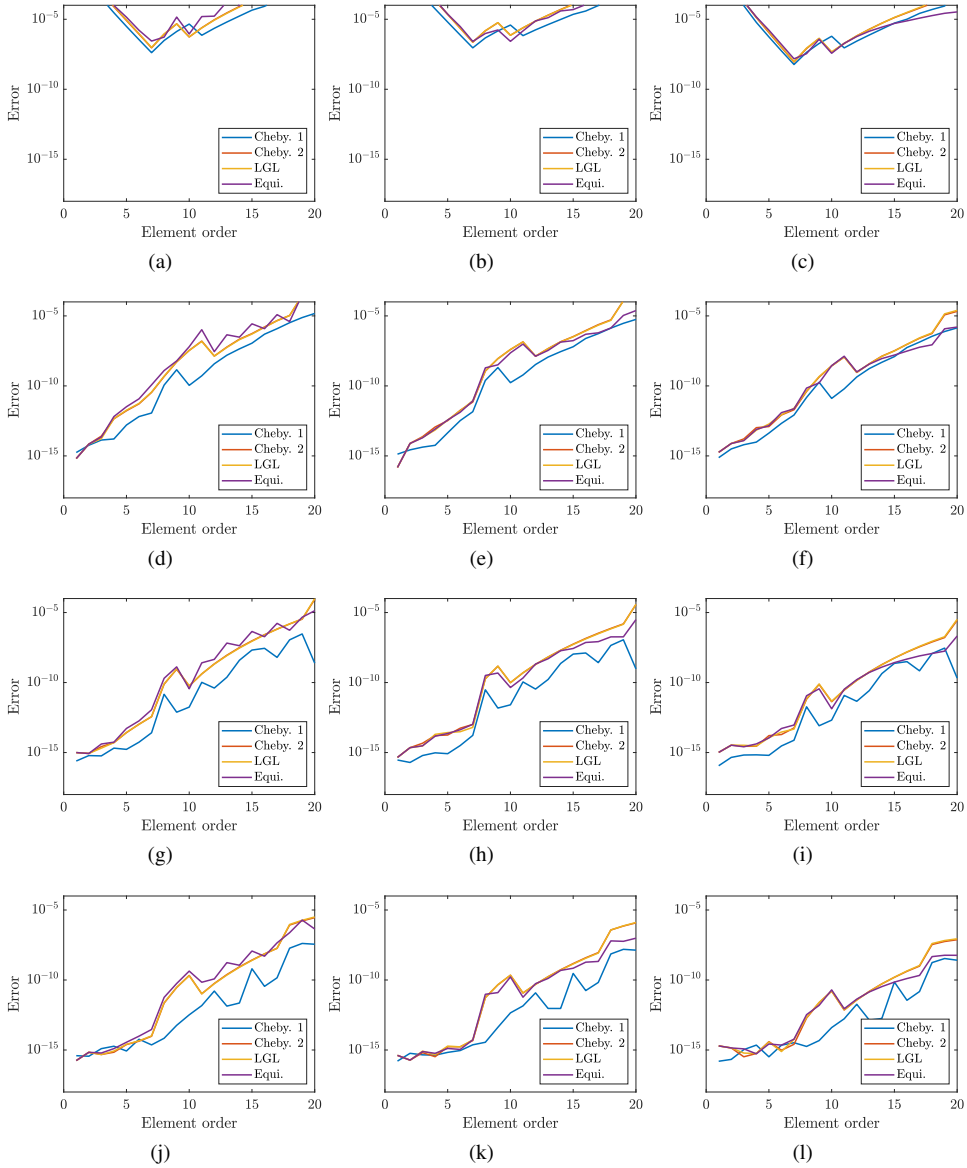

Figure 1: L_2 scaled error ϵ_2 in the computation of integrals (a, d, g, j) I_1, (b, e, h, k) I_2, and (c, f, i) I_3 using (a–c) $M = 2(p+1)$, (d–f) $M = 3(p+1)$, (g–i) $M = 4(p+1)$ and (j–l) $M = 8(p+1)$ integration points.

The Bézier–Bernstein space is used to describe the exact element geometry as $\Gamma^j(\mathbf{x}) = \mathbf{r}_n^j(t)$. Therefore, the integrals of the elements in eqn (2) are rewritten on the univariate basis $t \in [0,1]$ as [4], [11]:

$$\int_{\Gamma^j} f(\mathbf{x},\xi)\, d\Gamma = \int_0^1 f(\mathbf{x}(t),\xi) \left| \frac{d\mathbf{r}_n^j(t)}{dt} \right| dt, \tag{22}$$

where $f(\mathbf{x}, \xi)$ represents the integration kernel. Furthermore, eqn (22) can be transformed into the integration interval $[-1, 1]$ to employ the proposed quadrature rules.

The BEM formulation in the Bézier–Bernstein space employs the Lagrange interpolant relative to the Bernstein basis for the field variable approximation to an element [12]. The field approximation given by the shape function interpolates $n+1$ nodal values through the element shape functions ϕ^i of order n, for $i = 0, \ldots, n$ (eqn (3)). Then, the field approximation becomes:

$$u(t) = \sum_{i=0}^{p} \phi^i(t) u^i = \sum_{i=0}^{p} \left\{ \sum_{k=0}^{n} c_k^i B_k^n(t) \right\} u^i = \sum_{i=0}^{p} R^i(t, \ldots, t) u^i, \tag{23}$$

where the evaluation of the element shape function $\phi^i(t)$ also benefits from the computational advantages of using the polar form $R^i(t_1, \ldots, t_n)$ according to eqn (20). Once the geometry and the field approximation given by eqns (21) and (23) are introduced in eqn (2), the boundary integrals are computed using a standard Gauss–Legendre quadrature with $p+1$ integration points whenever the collocation point is sufficiently distant from the integration element. Otherwise, the solution of singular or weakly singular integrals is numerically computed using the proposed quadrature rules when the collocation point belongs to the integration element or using a smoothing transformation [4], [5].

3 BENCHMARK PROBLEM

In this section, we analyze the performance of the proposed method by applying it to an elastodynamic boundary value problem, consisting of an infinite length cylindrical cavity with radius 1 m in a full space [13]. This problem can be solved using a two-and-a-half-dimensional approach as the geometry is invariant in the longitudinal direction z.

The full space is characterized by the shear wave velocity $C_s = 150$ m/s, dilatational wave velocity $C_p = 300$ m/s, density $\rho = 1{,}800$ kg/m^3, and a material damping ratio $\beta_s = \beta_p = 0.05$ in both deviatoric and volumetric deformation.

The cavity is subjected to a longitudinally harmonic internal pressure $\tilde{p}(\kappa_z, \omega) = 1$ with wavelength $\lambda_z = 2\pi/k_z$ and frequency ω. This load produces a harmonic longitudinal radial displacement that is axisymmetric around the z axis, with the same wavelength as the load.

In this work, the circular shape was approximated by cubic Bézier curves. Four patches were used to define the boundary geometry with the control polygon represented in Fig. 2. The patches were discretized into a number of boundary elements ensuring $\kappa_s h = 3$ and a nodal density per wavelength $d_\lambda = 2\pi p/\kappa_s h = 12$, where $\kappa_s = \omega/C_s$ and p is the order of the elements.

The Green's functions in an elastic unbounded medium are obtained in 2.5D from the derivation of two potentials for the irrotational and equivoluminal parts of the displacement vector [14], that are given in terms of the Hankel functions of the second kind $H_0^{(2)}(kr)$, where k is either the wavenumber related to dilatational or shear waves and r is the distance from the source to the observation point. The Hankel function has a logarithmic singularity given by its series expansion at zero:

$$-\frac{\iota(2\log(kr) + \iota\pi + 2\gamma - 2\log(2))}{\pi} + O^2(kr), \tag{24}$$

where γ is the Euler–Mascheroni constant and the Greek letter ι represents the imaginary unit. This singularity is easily integrated by the proposed quadrature.

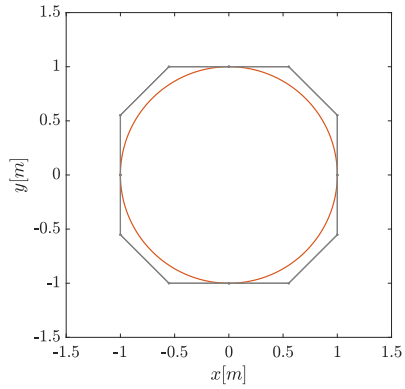

Figure 2: Cavity geometry using four cubic Bézier curves. Control points and their related control polygons are represented by grey circles and grey lines.

Fig. 3 shows the radial displacements at a distance 10 m from the cavity centre. The problem solution was computed for a frequency range from 1 to 100 Hz and a dimensionless wavenumber $\bar{\kappa}_z = \kappa_z C_s/\omega = 1$. The obtained results are in good agreement with the analytical and numerical solutions given in François et al. [13] and Forrest and Hunt [15], [16].

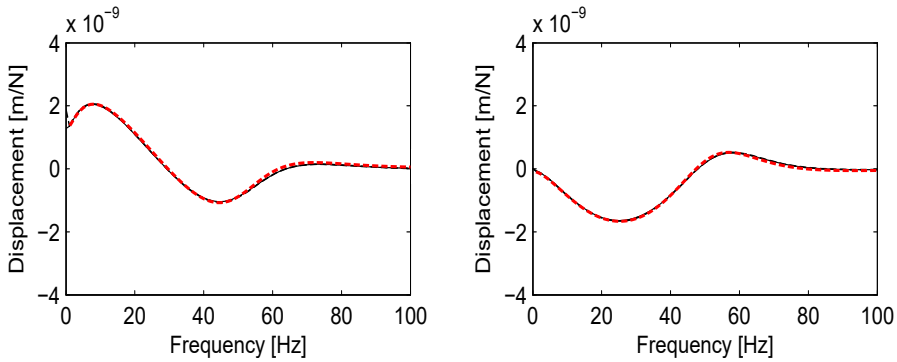

Figure 3: (a) Real; and (b) Imaginary parts of the radial displacement at a distance 10 m from the center of the cavity. Comparison of computed results (red line) and reference solutions (black line) [13], [15], [16].

4 CONCLUSIONS

This paper has proposed a new quadrature rule to assess singular kernels in the BIE. The quadrature rule is valid for common engineering problems that exhibit weakly singular and singular behaviors (acoustics, elastostatic, elastodynamic, heat transfer). The proposed method allowed for the accurate integration of kernels of arbitrary order and node distributions. The generality of the method is achieved because the element shape functions

can be derived from the Bernstein basis. The proposed procedure has been verified by the solution of a 2.5D elastodynamic problem.

ACKNOWLEDGEMENTS

The authors would like to acknowledge the financial support provided by the Spanish Ministry of Science and Innovation under the research project PID2019-109622RB-C21, and US-126491 funded by the FEDER Andalucía 2014–2020 Operational Program. The support of the Andalusian Scientific Computing Centre (CICA) is gratefully acknowledged.

REFERENCES

[1] Cheng, A.H.D. & Cheng, D.T., Heritage and early history of the boundary element method. *Engineering Analysis with Boundary Elements*, **29**(3), pp. 268–302, 2005.
[2] Domínguez, J., *Boundary Elements in Dynamics*, Computational Mechanics Publications and Elsevier Aplied Science, 1993.
[3] Carley, M., Numerical quadratures for singular and hypersingular integrals in boundary element methods. *SIAM Journal on Scientific Computing*, **29**(3), pp. 1207–1216, 2007.
[4] Romero, A., Galvín, P., Cámara-Molina, J. & Tadeu, A., On the formulation of a bem in the Bézier–Bernstein space for the solution of Helmholtz equation. *Applied Mathematical Modelling*, **74**, pp. 301–319, 2019.
[5] Monegato, G. & Scuderi, L., Numerical integration of functions with boundary singularities. *Journal of Computational and Applied Mathematics*, **112**(1), pp. 201–214, 1999.
[6] Kolm, P. & Rokhlin, V., Numerical quadratures for singular and hypersingular integrals. *Computers and Mathematics with Applications*, **41**(3), pp. 327–352, 2001.
[7] Patera, A.T., A spectral element method for fluid dynamics: Laminar flow in a channel expansion. *Journal of Computational Physics*, **54**(3), pp. 468–488, 1984.
[8] Brandao, M.P., Improper integrals in theoretical aerodynamics – the problem revisited. *AIAA Journal*, **25**(9), pp. 1258–1260, 1987.
[9] Romero, A., Galvín, P. & Tadeu, A., An accurate treatment of non-homogeneous boundary conditions for development of the BEM. *Engineering Analysis with Boundary Elements*, **116**, pp. 93–101, 2020.
[10] Ramshaw, L., Blossoming: A connect-the-dots approach to splines. Digital Equipment Corporation SRC Report No. 19, 1987.
[11] Seidel, H.P., An introduction to polar forms. *IEEE Computer Graphics and Applications*, **13**(1), pp. 38–46, 1993.
[12] Farouki, R.T., Goodman, T. & Sauer, T., Construction of orthogonal bases for polynomials in Bernstein form on triangular and simplex domains. *Computer Aided Geometric Design*, **20**(4), pp. 209–230, 2003.
[13] François, S., Schevenels, M. & Degrande, G., *BEMFUN: MATLAB Toolbox for Boundary Elements in Elastodynamics*, Katholieke Universiteit: Leuven, 2009.
[14] Tadeu, A. & Kausel, E., Green's functions for two-and-a-half-dimensional elastodynamic problems. *Journal of Engineering Mechanics*, **126**(10), pp. 1093–1097, 2000.
[15] Forrest, J. & Hunt, H., Ground vibration generated by trains in underground tunnels. *Journal of Sound and Vibration*, **294**(4), pp. 706–736, 2006.
[16] Forrest, J. & Hunt, H., A three-dimensional tunnel model for calculation of train-induced ground vibration. *Journal of Sound and Vibration*, **294**(4), pp. 678–705, 2006.